

Photoaffinity Probes

Detection of Bacterial Neutral Ceramidase in Diabetic Foot Ulcers with an Optimized Substrate and Chemoenzymatic Probes

Jiao Xia Zou, Wisely Chua, Zheng Ser, Shi Mei Wang, Grace Shu Hui Chiang, Kavitha Sanmugam, Boon Yeow Tan, Radoslaw M. Sobota, and Hao Li*

Abstract: Ceramidases (CDases) are important in controlling skin barrier integrity by regulating ceramide composition and affording downstream signal molecules. While the functions of epidermal CDases are known, roles of neutral CDases secreted by skin-residing microbes are undefined. Here, we developed a one-step fluorogenic substrate, **S-B**, for specific detection of bacterial CDase activity and inhibitor screening. We identified a non-hydrolyzable substrate mimic, **C6**, as the best hit. Based on **C6**, we designed a photoaffinity probe, **JX-1**, which efficiently detects bacterial CDases. Using **JX-1**, we identified endogenous low-abundance PaCDase in a *P. aeruginosa* monoculture and in a mixed skin bacteria culture. Harnessing both **S-B** and **JX-1**, we found that CDase activity positively correlates with the relative abundance of *P. aeruginosa* and is negatively associated with wound area reduction in clinical diabetic foot ulcer patient samples. Overall, our study demonstrates that bacterial CDases are important regulators of skin ceramides and potentially play a role in wound healing.

Introduction

Ceramides are a class of sphingolipids that constitute the majority of the lipid component in the stratum corneum (SC) of human skin.^[1] Together with cholesterol and free fatty acid, ceramides form the extracellular lipid lamellae which are essential for skin barrier integrity.^[2] Skin ceramides are heterogeneous; the majority of ceramides in the SC are the non-hydroxy and α -hydroxylated ceramides, while the ω -O-acylceramides are epidermis-specific and constitute approximately 10% weight of SC ceramides.^[3] Alterations to the ceramide composition and its associated metabolites have important consequences to the lipid lamellae structure and can alter skin barrier permeability implicated in dermatological diseases.^[4] In atopic dermatitis (AD), a chronic inflammatory cutaneous disease characterized by xerotic, pruriginous skin, there is a decrease in ceramide species such as acylceramides and *N*-acyl-6-OH dihydrosphingosine.^[5]

Ceramide composition in the SC is influenced by many lipid metabolism enzymes.^[1b,6] One important player in altering SC ceramides is the hydrolase ceramidase (CDase), which cleaves the amide bond between the sphingoid base and fatty acid.^[7] There are three classes of CDase—acid, neutral and alkaline; this classification is dependent on the pH optimum and catalytic mechanism of the enzyme. Besides having a direct effect on ceramide abundance, the metabolites generated have important roles in cellular signaling.^[8] Sphingosine and its metabolite sphingosine-1-phosphate can modulate keratinocyte proliferation and differentiation, and are important mediators of skin immunity and host antimicrobial defense.^[9] As such, the functions of skin-associated CDases have been heavily investigated.^[9,10] However, as the skin is resided by a community of microbes, it is important to consider the effect of microbe-secreted CDases and their effects on modifying the cutaneous environment.

Of all skin-associated microbes, only the secreted neutral ceramidase produced by the pathogen *Pseudomonas aeruginosa* has been studied. *P. aeruginosa* neutral ceramidase (PaCDase) first became of interest when AD skin culture isolates were found to have elevated CDase activity.^[11] PaCDase was subsequently purified from the *P. aeruginosa* clinical isolate AN17 obtained from an AD subject^[12] and the structure of this zinc metallo-enzyme was determined using the recombinant PaCDase.^[13] PaCDase is able to hydrolyze common ceramides and human SC-essential ω -O-acylceramides in vitro, and the hydrolysis of these ceramides

[*] J. X. Zou, Prof. Dr. H. Li
 Department of Chemistry, National University of Singapore
 3 Science Drive 3, Singapore 117543 (Singapore)
 E-mail: chmlihao@nus.edu.sg

W. Chua, Prof. Dr. H. Li
 Molecular Engineering Lab, Institute of Molecular and Cell Biology,
 Agency for Science, Technology and Research, Singapore
 61 Biopolis Drive, Proteos, Singapore 138673 (Singapore)

Dr. Z. Ser, S. M. Wang, Dr. R. M. Sobota
 Functional Proteomics Laboratory, Institute of Molecular and Cell
 Biology, Agency for Science, Technology and Research, Singapore
 61 Biopolis Drive, Proteos, Singapore 138673 (Singapore)

G. S. H. Chiang, K. Sanmugam, B. Y. Tan
 St Luke's Hospital, Singapore 659674 (Singapore)

© 2023 The Authors. Angewandte Chemie International Edition published by Wiley-VCH GmbH. This is an open access article under the terms of the Creative Commons Attribution Non-Commercial NoDerivs License, which permits use and distribution in any medium, provided the original work is properly cited, the use is non-commercial and no modifications or adaptations are made.

are promoted by glycerophospholipids derived from *Staphylococcus aureus*, an opportunistic pathogen that is highly abundant on AD-affected skin.^[14] By functioning as surfactants, these anionic lipids are likely to enhance ceramide hydrolysis by increasing the solubility of ceramides.^[14a] In a recent study utilizing a porcine model colonized with *P. aeruginosa*, higher loads of wound biofilm was observed in the sites colonized with the wildtype bacteria compared to the CDase knockout strain.^[15] Host lipids were found to induce PaCDase expression and this enzyme can further process the host ceramides, leading to the disruption of skin barrier integrity at the wound site. These studies highlight the potential role of bacterial CDase as a virulence factor and further investigation is required to establish whether bacterial CDases are involved in delayed wound healing, especially chronic wounds such as diabetic foot ulcers (DFU) which are often colonized by opportunistic pathogens,^[16] and represent a serious complication of diabetes.^[17]

The study of bacterial ceramidases is impeded by a lack of chemical tools to characterize the activity of neutral ceramidase, the only class of ceramidase in prokaryotes. Fluorescent ceramide analogs such as C12-NBD-ceramide require further isolation and purification for bacterial CDase activity quantification rendering it tedious.^[18] Currently, the only commercially available enzyme substrate RBM14C16, which was developed for human CDase originally and hydrolyzable by PaCDase, requires post-reaction addition of periodate to oxidize the aminodiol to umbelliferone (7-hydroxycoumarin), making real-time enzyme kinetics, high-throughput compound screening and in situ detection of bacterial ceramidases activity difficult.^[19] Furthermore, while several potent neutral ceramidase inhibitors have been identified against the human neutral ceramidase (nCDase),^[20] there is a paucity of such inhibitors for bacterial CDases. As small-molecule inhibitors are facile tools for chemical knockdown of enzyme activity,^[21] identifying such compounds will aid in studying the function of bacterial ceramidases.

In this work, we designed and synthesized one-step fluorogenic substrates (**S-A** and **S-B**) which can detect bacterial ceramidases activity efficiently. We used **S-B** to determine the enzyme kinetics of PaCDase and two previously uncharacterized CDase from *Corynebacterium*, a component of the skin microbiome.^[22] We observed that this fluorogenic substrate has specificity for the *P. aeruginosa* and *Corynebacterium jeikeium* ceramidases over the human nCDase. With this optimized substrate, we screened a small library of 63 compounds comprising of the zinc-chelating hydroxamates and substrate mimics of ceramidases. We identified C6-urea-ceramide (**C6**), a non-hydrolyzable substrate mimic, as a potent inhibitor of PaCDase. To convert **C6** to a chemoenzymatic probe for bacterial CDase profiling, we installed the photoactivatable diazirine motif and alkyne click-reaction handle at various positions and identified an optimized probe **JX-1**. Using this chemical toolbox, we were able to identify PaCDase in a complex protein mixture and mixed microbial community. Importantly, we were able to detect and quantify CDase from bacteria

cultures of diabetic foot ulcer samples. We observed a clear correlation of the CDase activity to *P. aeruginosa* relative abundance and wound area reduction, which suggests *P. aeruginosa* CDase's role as a virulence factor in DFU wound infections.

Results and Discussion

CDase fluorogenic substrate **S-B** enables real-time detection of bacterial CDase activity

To enable convenient, real-time determination of CDase enzyme kinetics, we first designed and synthesized two one-step Fluorescence Resonance Energy Transfer (FRET) CDase substrates. The backbones of both substrates were designed based on the commercial substrate RBM14C16 which has a shortened sphinganine-like chain with a long fatty acid chain (>10 C) important for enzyme affinity.^[18–19,23] (Figure 1A, S1A, Scheme S1). Given that both *N*-acyl-sphinganine and *N*-acyl-sphingosine can be hydrolyzed by PaCDase,^[12] we chose to modify the sphingosine chain instead of sphinganine (hydrogenated sphingosine) due to the easy installation of fluorophores through olefin metathesis.^[24] As the different fluorophore/quencher pairs may affect binding affinity, we adopted two relatively small size fluorophore/quencher pairs: 7-Methoxycoumarin-4-yl)acetyl (MCA)/2,4-dinitrophenyl (DNP) pair contained in **S-A**^[25] and 7-methoxycoumarin-3-carboxylate (MCC)/nitrobenzoxadiazole (NBD) in **S-B**.^[26] We observed hydrolysis of both substrates in 30 min (**S-A**) and 20 mins (**S-B**) by recombinant *P. aeruginosa* ceramidase (rPaCDase, expressed with solubility tag NT11) (Figure 1B and S1C), with **S-B** being the optimal substrate with a V_{\max} of 750.1 pmol/min (Figure 1D).

To compare the enzymatic activity of skin-associated bacterial neutral ceramidases with human nCDase, we recombinantly expressed the putative nCDases from two common skin commensals *Corynebacterium amycolatum* (rCaCDase) and *Corynebacterium jeikeium* (rCjCDase), in addition to rPaCDase. All recombinant proteins were expressed with the NT11 (sequence: VSEPHDYNYEK) solubility tag as this increases solubility and protein yield of the recombinant enzyme (Figure 1C).^[27] We then determined the optimal pH for rPaCDase, rCaCDase and rCjCDase (Figure S1B, approximately 6.8, 9.5, 7.5 respectively) and used this optimized assay condition to determine the enzyme kinetics of these 3 CDases with **S-B** (Figure 1D, 1E, and S1E). We observed that rCjCDase strongly hydrolyzed **S-B** with a V_{\max} of 172.2 pmol/min (Figure 1E). In contrast, the putative CDase from *C. amycolatum* has weak activity towards the substrate (V_{\max} of 4.473 pmol/min, Figure S1E) and this was also observed for **S-A** (Figure S1C) and the commercial substrate RBM14C16. Interestingly, while RBM14C16 was hydrolyzed by rPaCDase and rCjCDase at a rate comparable to the human recombinant nCDase,^[19] **S-B** was preferentially hydrolyzed by both bacterial CDases. The V_{\max} for **S-B** hydrolysis was 40-fold and 9-fold higher for rPaCDase and rCjCDase respectively

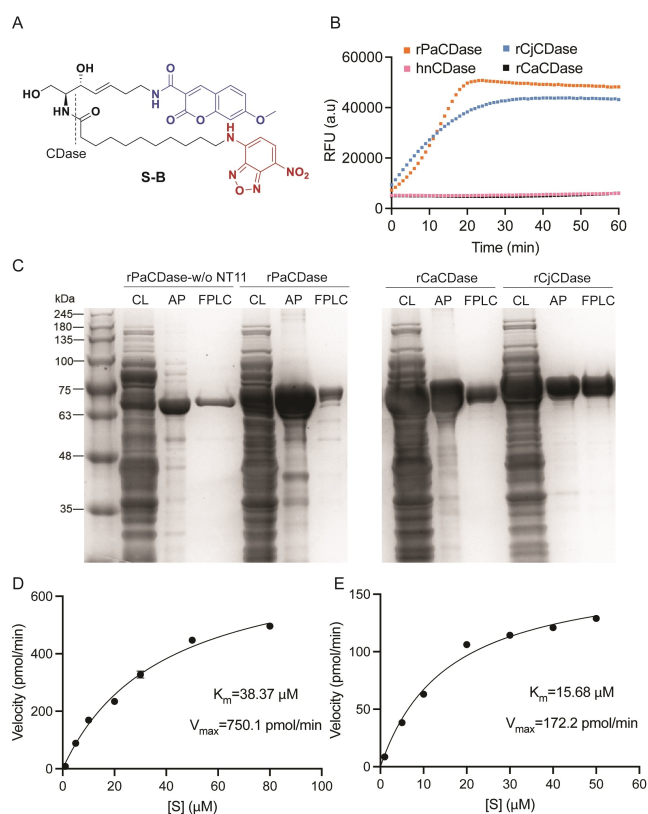


Figure 1. Design, synthesis and characterization of CDase substrates in three microbial CDases and human neutral CDase. A) Structure of substrate **S-B**. B) Progress curve of **S-B** hydrolysis for three bacterial CDases and recombinant human neutral CDase in 60 min. Plotted values were shown as median fluorescence intensity of three replicates. 200 ng enzymes were used. C) SDS-PAGE showing the purification of three recombinant neutral ceramidases from *Pseudomonas aeruginosa*, *Corynebacterium amycolatum*, and *Corynebacterium jeikeium* respectively. rPaCDase, rCjCDase and rCaCDase were expressed with 6xHis tag as well as NT11 fusion tag (sequence = VSEPHDYNIEK). CL: cell lysate of CDase-expressing *E. coli*; AP: pooled fractions after affinity purification; FPLC: pooled fractions after FPLC. The left panel shows recombinant PaCDase without (w/o) or with NT11 fusion tag. The right panel shows rCjCDase and rCaCDase. D) and E) Michaelis–Menten plot of rPaCDase and rCjCDase respectively, determined by using **S-B** as a substrate. Plotted values are shown as mean with standard deviation, $n=2$ technical replicates. Michaelis–Menten constant (K_m) and maximal velocity (V_{max}) of **S-B** hydrolysis for each enzyme are shown.

when compared to the human nCDase (V_{max} of 19.00 pmol/min, Figure S1F). The preferential hydrolysis of **S-B** by rPaCDase indicates that important differences exist in the substrate binding pocket of the bacterial and human neutral ceramidase.

Screening and design of bacterial CDase inhibitors

As our developed substrate **S-B** affords easy access to high throughput chemical screen using enzyme assay, we set out to identify bacterial CDases inhibitors, of which only a handful of weak inhibitors such as ceramidastin (IC_{50} value

of 12 μM)^[28a] and citric acid (IC_{50} value of 102 μM)^[28b] have been identified. We focused on a small library of 63 compounds comprising of hydroxamates which inhibit Zn-dependent metalloenzymes due to its ability to chelate the zinc critical for enzyme activity,^[29] substrate mimics and previously reported human CDase inhibitors (Figure 2, Table S1).^[20,30–31] We first screened these compounds at 200 μM against rPaCDase and identified 4 compounds with more than 80% inhibition (Figure 2A and 2B). We then determined the dose-response curves of these top 4 compounds. Of these, the most potent compound is the substrate mimic C6-urea-ceramide (**C6**) with an IC_{50} of 4.12 μM, followed by another substrate mimic sphingosine (IC_{50} of 9.86 μM) and the hydroxamate MC1568 (IC_{50} of 37.99 μM) (Figure 2C and D). Some well-studied human nCDase inhibitors such as DP-24a, B13 and KP-77^[30–31] bear little or no inhibitory effects on rPaCDase activity at 200 μM (Table S1). Our inhibitor screening further demonstrates that PaCDase may prefer distinct inhibitor scaffolds due to the differences in the enzyme's substrate binding pocket as reported in previous studies.^[13,32]

Design, synthesis and activity evaluation of CDase affinity-based photoreactive probes (AfBPs)

With **C6** identified as a potent inhibitor of rPaCDase, we further modified this compound to generate a clickable chemoenzymatic probe for CDase profiling. Activity-based probes for acid ceramidase have been previously

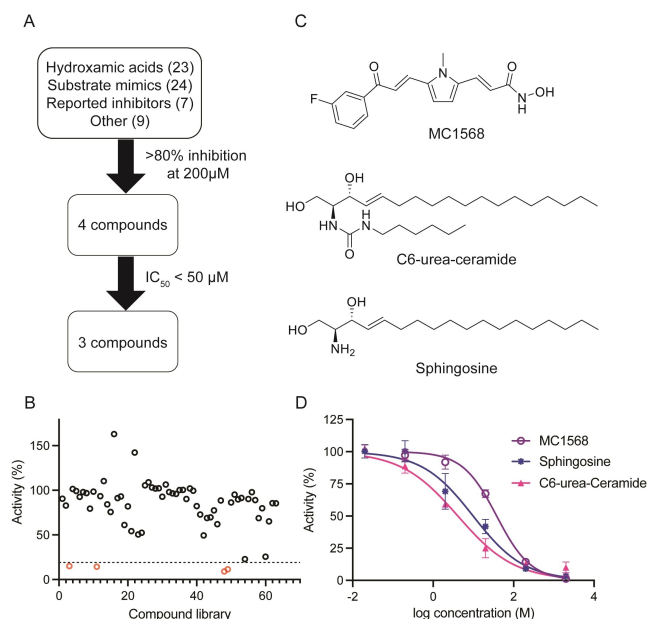


Figure 2. Screen and design of CDase inhibitors. A) Flow chart of compound library screening. B) rPaCDase activity in the presence of each inhibitor in the library. Compounds were screened at 200 μM. Plotted values were shown as mean without error bar ($n \geq 2$). C) Structures of top 3 inhibitors of rPaCDase. D) Dose-response curves of top 3 inhibitors of rPaCDase using **S-B** as a substrate. Plotted values shown as mean with standard deviation ($n=3$).

developed^[33] as this class of CDase has an active site cysteine as a nucleophile for covalent attachment of the probe's electrophilic warhead.^[34] However, neutral ceramidases are Zn-dependent metalloenzymes where a molecule of water serves as the nucleophile in hydrolysis.^[13,32] Therefore we adopted an affinity-based approach by modifying **C6** at various positions with the photoreactive diazirine and an alkyne handle for further Click-reaction modifications. 5 AfBPs (**JX-1-5**, Figure 3A) were designed with the diazirine and alkyne installed at different positions of two alkyl chains (sphingosine-chain and amino-chain) as positions of the photoreactive group can affect labeling efficiency and specificity.^[35] **JX-1** and **-2** were designed to have the photoreactive diazirines in the middle or terminal end of their amino chain, whereas the photoreactive diazirines were installed at the sphingosine-chain for **JX-3** and **5**. **JX-4** possesses an extra diazirine group compared to **JX-3** and was designed to determine whether more diazirine groups would enhance labeling efficiency. The probes were synthesized according to the synthetic routes shown in Scheme S2.

We first evaluated their binding affinities by determining the IC_{50} against rPaCDase activity (Figure 3B). We observed that **JX-1** and **3** exhibit good inhibitory activity, with IC_{50} values at 4.1 μ M and 5.4 μ M respectively, similar to the parent inhibitor **C6** (4.1 μ M). Compared to **JX-3**, **JX-4** which contains one additional diazirine group shows more than 2-fold increase in its IC_{50} value. **JX-5** showed the weakest inhibition with IC_{50} of 88.2 μ M, likely due to the long sphingosine chain or ester group interfering with active site binding.

Probe JX-1 shows high CDase labeling efficiency and selectivity in complex protein mixture

We then assessed the ability of the most potent probe **JX-1** to label bacterial CDases. We first optimized the conditions for **JX-1** labeling in purified rPaCDase. After incubation of the probe with recombinant CDase followed by UV irradiation, we added TAMRA-azide along with the neces-

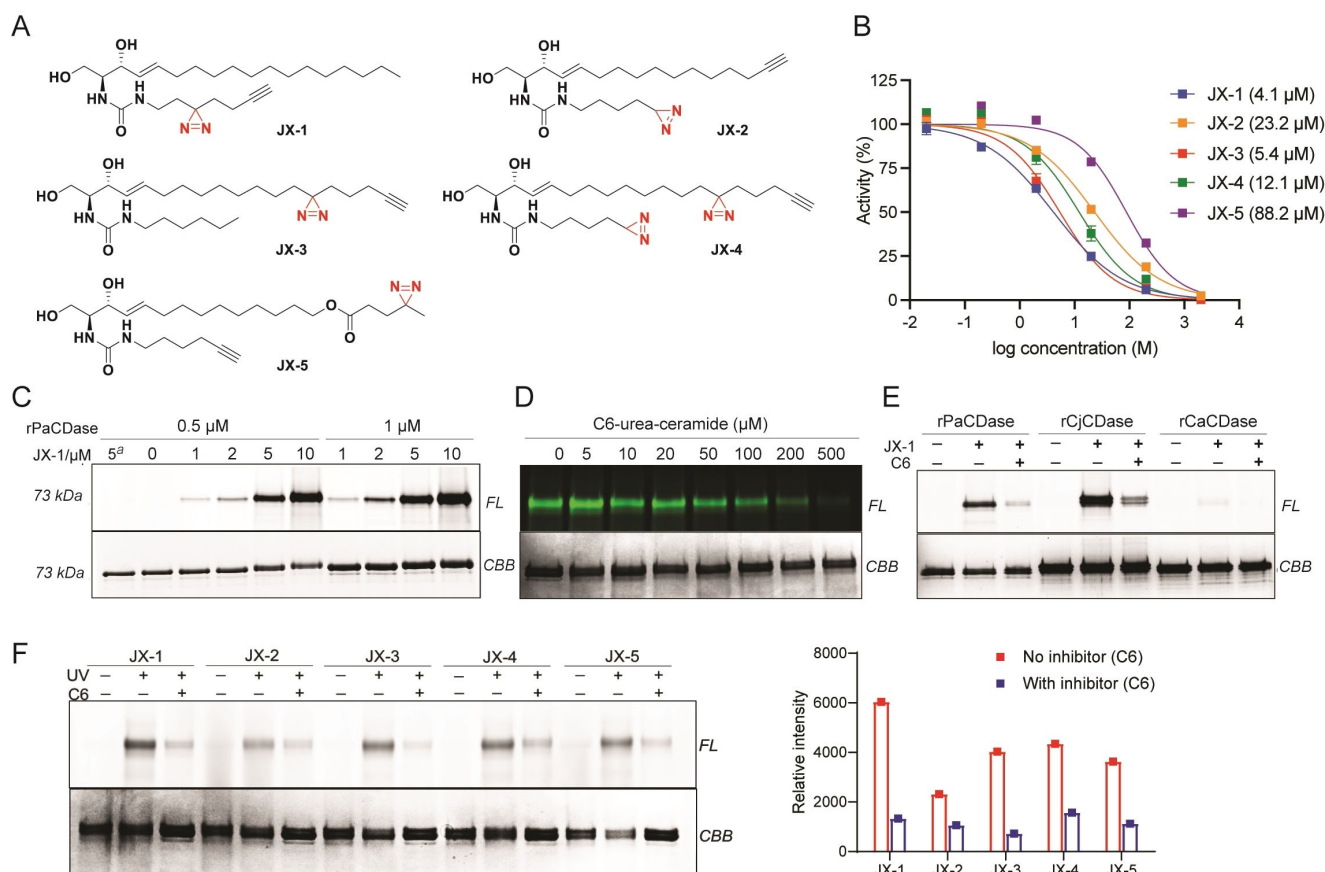


Figure 3. Design and application of AfBPs for bacterial CDase characterization. A). Structures of 5 AfBPs. B) IC_{50} curve of 5 AfBPs as assessed by inhibition of rPaCDase. Concentrations shown in the legend are corresponding IC_{50} values. Plotted values shown as mean with standard deviation ($n=3$). C) Labeling of rPaCDase (0.5 or 1 μ M) using varying concentrations of **JX-1**.^a: no UV irradiation at 365 nm. D) Inhibitor competition assay with varying concentrations of C6-urea-ceramide (**C6**). Experiment was performed using 0.5 μ M purified rPaCDase, 5 μ M probe, 20 min UV irradiation at 365 nm. E) **JX-1** labeling of three bacterial recombinant CDases with 0.5 μ M purified CDase, 5 μ M probe, 20 min UV irradiation at 365 nm. **C6** is used at 200 μ M. F) Comparison of labeling efficiency of 5 AfBPs in purified rPaCDase with or without **C6** inhibitor competition. All labeling profiles were assessed by SDS-PAGE and in gel fluorescence analysis. Protein band intensities were quantified using ImageJ (right panel). FL = in-gel fluorescence, CBB = Coomassie brilliant blue.

sary Click reaction reagents. The labeled proteins were then resolved by sodium dodecyl-sulfate polyacrylamide gel electrophoresis (SDS-PAGE) with probe labeling visualized by fluorescence scan at Ex/Em 532/580. In purified CDase, we observed that labeling occurs when the concentration of **JX-1** was as low as 1 μM and a short UV irradiation is sufficient for labeling (Figure 3C and S2A). To determine whether the labeling is specific, we pretreated the enzyme with the parent inhibitor **C6** followed by probe labeling. We observed 500 μM of **C6** is able to completely abrogate labeling of rPaCDase by **JX-1** (Figure 3D). Furthermore, **JX-1** can label both rCjCDase and rCaCDase, and this labeling can be competed off with 200 μM of **C6** (Figure 3E). However, we observed only weak labeling of rCaCDase and this corresponds to our previous observation that this putative ceramidase has low enzymatic activity towards the synthetic substrates (Figure 1B and S1).

With the optimized probe labeling conditions, we compared the labeling efficiency of the 5 probes towards purified rPaCDase. To this end, rPaCDase was incubated with 5 μM AfBPs in the presence or absence of UV and competitor (Figure 3F). Similar to the inhibition assay, we observed that **JX-1** demonstrates the strongest labeling intensity among these probes. To determine the selectivity of probe labeling, we performed the same labeling experiment using cell lysates derived from *E. coli* overexpressing rPaCDase or rCjCDase. We observed that **JX-1** shows the best selectivity for labeling of CDase in this complex protein

mixture (Figure S3). Overall, **JX-1** demonstrates the highest probe labeling efficiency and enzyme selectivity among our small panel of CDase probes. However, **JX-1** is not selective for bacterial CDase as it is capable of labeling human neutral CDase (Figure S2B).

Chemoenzymatic probe **JX-1** labels low-abundance endogenous PaCDase in *P. aeruginosa* secretome

We next investigated whether our optimized chemoenzymatic probe **JX-1** can be used to detect native secreted bacterial CDase. As PaCDase is not constitutively expressed in *P. aeruginosa*, we first determined the conditions for optimal CDase production in culture. We observed the presence of native PaCDase in each cell fraction of *P. aeruginosa* PAO1 grown in BHI medium supplemented with or without sphingosine. Consistent with previous studies showing the effect of sphingosine in inducing CDase expression in *P. aeruginosa*,^[36] we detected a clear increase in CDase activity in the extracellular fraction in the presence of sphingosine (Figure 4A). This corresponds to a decrease in the CDase detected in the intracellular fraction, indicating that sphingosine stimulates production and secretion of the intracellular CDase. Next, we incubated supernatants of *P. aeruginosa* PAO1 culture in BHI medium with or without sphingosine with **JX-1**, followed by in situ Click reaction with TAMRA-azide. As shown in Figure 4B, a protein band

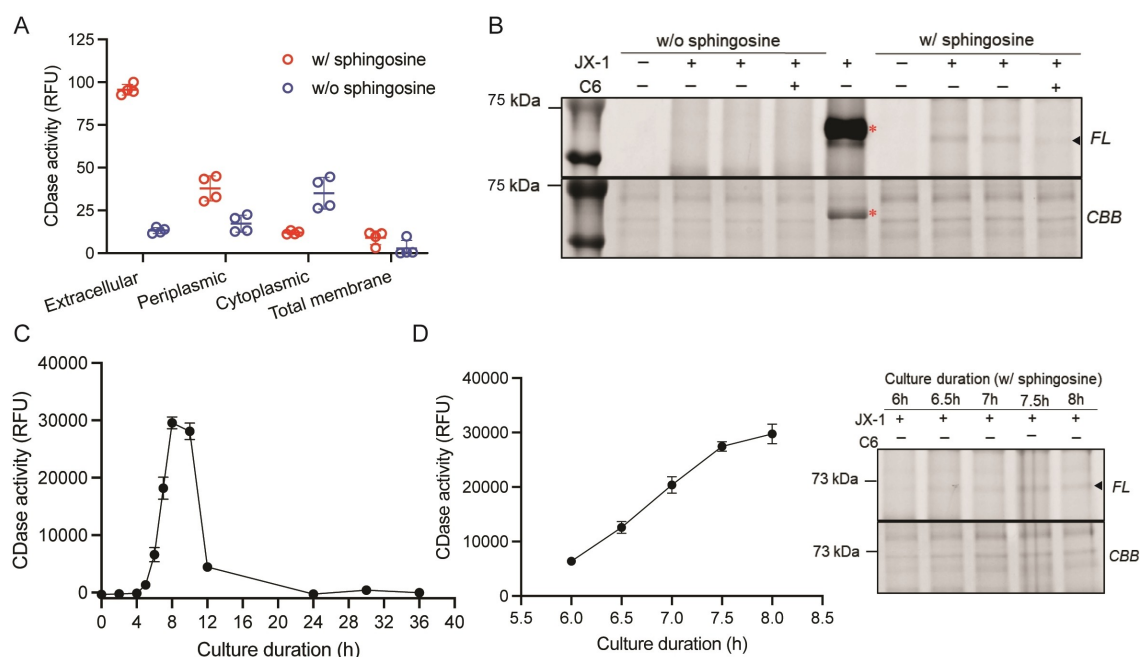


Figure 4. Application of AfBP and substrate to complex protein mixture. A) CDase activity of *P. aeruginosa* PAO1 cell fractions. Plotted values shown as mean with standard deviation ($n=4$). 200 μM sphingosine were supplemented in culture medium BHI where indicated. B) **JX-1**-TAMRA labeling of culture supernatant of *P. aeruginosa* PAO1 supplemented with or without 200 μM sphingosine. 200 μL culture supernatant, 50 μM **JX-1**, and 0.5 mM **C6** used. Asterisk*: purified rPaCDase spiked (73.2 kDa). Arrow indicates expected size of PaCDase. C) CDase activity of culture supernatant of *P. aeruginosa* PAO1 supplemented with sphingosine from 0–36 h. D) **JX-1**-TAMRA labeling (right panel) and the corresponding CDase activity (left panel) of *P. aeruginosa* PAO1 culture supernatant at 6–8 h of growth. 200 μL culture supernatant, 50 μM **JX-1**, and 0.5 mM **C6** used. Plotted values shown as mean with standard deviation.

with molecular weight around 71 kDa is detected after in-gel fluorescence scan and this labeling is competed away by addition of the inhibitor **C6**. In culture supernatants of *P. aeruginosa* PAO1 culture without sphingosine induction, we did not detect CDase activity and this protein band (Figure 4B). We then obtained the culture supernatant at various time points of *P. aeruginosa* PAO1 planktonic culture and determined the presence of native CDase using the substrate **S-B** and probe **JX-1**. From the enzyme activity assay, we observed that CDase activity is detected after 6 h of culture, peaks around 8 h and decreases thereafter (Figure 4C and 4D). Consistent with the activity assay, the protein band around 71 kDa is only detected when there is considerable CDase activity (Figure 4D, S4). We further performed avidin-biotin pull-down assay using **JX-1** clicked with azide-biotin and verified that both recombinant and endogenous PaCDase in complex mixture were successfully labeled (Figure S5). Finally, to confirm the identity of this protein, we performed in-gel digestion of this 71 kDa gel band followed by mass spectrometry proteomics and determined that PaCDase was indeed present in this protein band (Table S2). Overall, both the optimized substrate and probe are facile chemical tools to detect and quantify the low abundant native CDase in a complex protein mixture.

CDase activity in complex microbial community and wound cultures

We next wanted to assess whether the probe can detect CDase present in a complex microbial community. To this end, we cultured a synthetic community of skin-associated bacteria comprising of *P. aeruginosa* ATCC 15692, *Staphylococcus aureus* ATCC 25904, *Staphylococcus epidermidis* ATCC 14990, *Enterococcus faecalis* ATCC 47077 and *Corynebacterium striatum* ATCC 6940 in the presence or absence of sphingosine. After 8 hours of culture, we obtained the extracellular media from this mixed culture and incubated it with **JX-1**. Of these strains, only *P. aeruginosa* contains the gene for CDase expression. We observed that PaCDase in the mixed microbial culture supernatant was successfully labeled by **JX-1** when sphingosine was supplemented, and the labeling is abrogated in the presence of **C6** inhibitor (Figure 5A).

After determining that our optimized probe and substrate can be used to detect and quantify bacterial CDase activity in a mixed microbial background, we sought to use these tools to assess bacteria-associated CDase activity in wound culture samples obtained from DFU patients. We recruited 29 patients with DFU and obtained wound swabs from them weekly over a 4-week period. Wound characteristics including wound area were recorded at each sampling. We then cultured the swabs obtained at week 1 in BHI media in the presence of sphingosine and assessed for

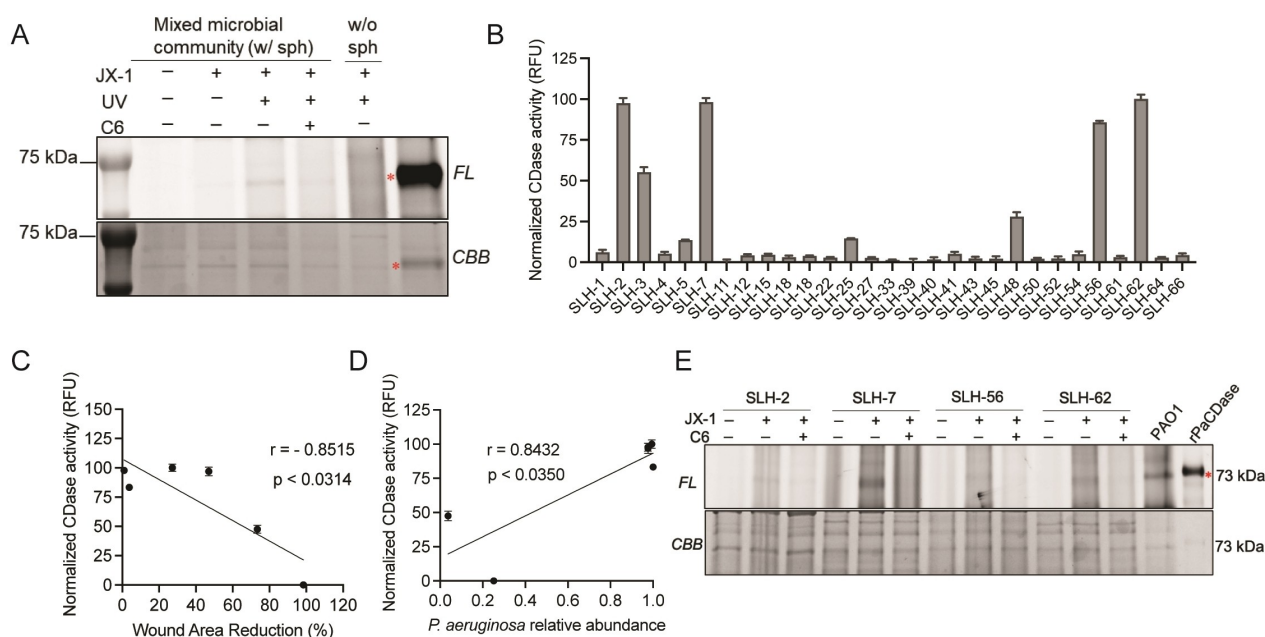


Figure 5. Application of bacterial CDase AfBP and substrate to detect CDase in complex microbial community. A) **JX-1**-TAMRA labeling of known mixed microbial culture supernatant supplemented with or without 200 μ M sphingosine. 200 μ L culture supernatant, 50 μ M **JX-1**, and 0.5 mM **C6** used. The mixed microbial community consists of *P. aeruginosa* ATCC 15692, *S. aureus* ATCC 25904, *S. epidermidis* ATCC 14990, *E. faecalis* ATCC 47077, *C. striatum* ATCC 6940. Asterisk*: purified rPaCDase spike-in (73.2 kDa). B) CDase enzyme activity in DFU clinical culture samples. Plotted values shown as mean with standard deviation ($n=3$). C) Correlation of CDase activity with wound area reduction from week 1 to week 4. D) Correlation of CDase activity to *Pseudomonas aeruginosa* abundance. For both C and D, $n=6$ patient samples and Pearson correlation coefficient (r) and p -value were determined by GraphPad Prism 8. E) **JX-1**-TAMRA labeling of DFU samples with positive CDase activity. 200 μ L culture supernatant, 50 μ M **JX-1**, and 0.5 mM **C6** used.

CDase activity using substrate **S-B** and probe **JX-1**. We detected strong CDase activity in 4 samples (SLH-2, 7, 56, 62), while 2 samples had weak but detectable activities (SLH-3 and 48) (Figure 5B). Next, we correlated bacterial CDases activity with wound area for the 6 samples with detectable CDase activity (SLH-2, 3, 7, 25, 56, 62; SLH-48 not recorded at week 4) (Figure C, S5A). We observed that bacterial CDase activity at week 1 is negatively correlated with wound area reduction from week 1 to week 4 (Figure 5C, $r = -0.8515$, $p = 0.0314$). This enzyme activity also has a positive ($r = 0.6985$, $p = 0.1226$), though not statistically significant correlation with wound area at week 4 (Figure S6A). These results suggest that bacterial CDases can potentially impact wound healing.

To decipher which bacteria species are responsible for secreting the CDase, we extracted the DNA from the wound swab cultures that possess CDase activity and sequenced the bacteria community using full length 16S PacBio sequencing. We observed that *Pseudomonas aeruginosa* is the only common bacteria species existing in all 6 samples (Figure S6B). Using Pearson correlation, we determined that *P. aeruginosa* abundance is positively ($r = 0.8432$, $p = 0.0350$) correlated with CDase activity (Figure 5D), suggesting that the CDase activity is from *P. aeruginosa*. To further validate this, 4 DFU culture samples (SLH-2, 7, 56, 62) were subjected to **JX-1-TAMRA** labeling. We observed the presence of a protein band around 71 kDa in the gel, similar in molecular weight to the CDase previously observed in *P. aeruginosa* PAO1 induction and protein labeling was reduced in the presence of the **C6** inhibitor. (Figure 5E). We performed in-gel digestion followed by LC-MS proteomics analysis and validated the presence of *P. aeruginosa* CDase across those 4 DFU samples (Table S2). Taken together, these results suggest the potential roles of skin-residing microbial CDase as a virulence factor in diabetic wound infections. While further studies are required to demonstrate *P. aeruginosa* CDase potentially interfering with wound healing in DFU, we postulate that this extracellular bacterial CDase can dramatically change the wound environment through degradation of ceramide, the key barrier lipid. The resulting sphingosine and downstream metabolite sphingosine-1-phosphate could have extensive effects on keratinocyte proliferation and migration, affecting wound closure.^[9]

Conclusion

Bacterial CDases, especially those produced by microbes that are part of the human microbiome, can have profound effects on shaping the host environment. However, studies on their functional roles and impact on the host is impeded by the lack of chemical tools. In our study, we designed and synthesized one-step bacterial CDase substrates for fast CDase detection and inhibitor screening, and, to our knowledge, the first affinity-based probes for CDase. The optimized chemoenzymatic probe **JX-1** is capable of bacterial CDase labeling, identification and quantification in complex microbial communities. Finally, using both the substrate and probe, we observed a clear association

between bacterial CDase activity, *P. aeruginosa* abundance and wound area reduction. Our study thus highlights the importance of considering the role of bacterial CDases produced by microbes residing on human skin and how these enzymes can modify the environment they reside in. We envision that **JX-1** combined with affinity enrichment or fluorescent labeling can be useful in identifying ceramidases produced by different bacteria for further functional elucidation of these enzymes. In addition, the use of inhibitors that selectively target bacterial CDases has the potential to serve as a therapeutic approach in combination with antibiotics, promoting the healing process of infected wounds.

Acknowledgements

H.L. acknowledges support from the MOE AcRF Tier 1 grant (R-143-000-B79-114 and R-143-000-C16-114), Wound Care Innovations for the Tropics Program, A*STAR Industry Alignment Fund-Pre-Positioning grant (H19/01/a0/0GG9) and Singapore Ministry of Health's National Medical Research Council (MOH-000612-00). R.M.S. acknowledges support from A*STAR Core funding awarded by the Biomedical Research Council of the Agency for Science, Technology and Research (A*STAR). Z.S. acknowledges support from A*STAR career development award and by an A*STAR Young Achiever's Award. The authors are grateful for the support of research coordinators and support staff from St Luke's Hospital.

Conflict of Interest

The authors declare no conflict of interest.

Data Availability Statement

The data that support the findings of this study are available in the supplementary material of this article.

Keywords: Bacterial Ceramidase · Enzyme Substrates · Inhibitors · Photoaffinity-Based Probes · Wound Infection

- [1] a) H. J. Yardley, R. Summerly, *Pharmacol. Ther.* **1981**, *13*, 357–383; b) A. Kihara, *Prog. Lipid Res.* **2016**, *63*, 50–69; c) M. Suzuki, Y. Ohno, A. Kihara, *J. Lipid Res.* **2022**, *63*, 100235.
- [2] a) L. Coderch, O. López, A. de la Maza, J. L. Parra, *Am. J. Clin. Dermatol.* **2003**, *4*, 107–129; b) L. Norlén, M. Lundborg, C. Wennberg, A. Narangifard, B. Daneholt, *J. Invest. Dermatol.* **2022**, *142*, 285–292.
- [3] a) L. Opálka, A. Kovacik, P. Pullmannova, J. Maixner, K. Vavrova, *J. Lipid Res.* **2020**, *61*, 219–228; b) H. Yamamoto, M. Hattori, W. Chamulitrat, Y. Ohno, A. Kihara, *Proc. Natl. Acad. Sci. USA* **2020**, *117*, 2914–2922; c) L. Opálka, J. M. Meyer, V. Ondrejcekova, L. Svatosova, F. P. W. Radner, K. Vavrova, *J. Lipid Res.* **2022**, *63*, 100226.

- [4] a) S. Borodzicz, L. Rudnicka, D. Mirowska-Guzel, A. Cudnoch-Jedrzejewska, *Lipids Health Dis.* **2016**, *15*, 13; b) M. Danso, W. Boiten, V. van Drongelen, K. Gmelig Meijling, G. Gooris, A. El Ghalbzouri, S. Absalah, R. Vreeken, S. Kezic, J. van Smeden, S. Lavrijsen, J. Bouwstra, *J. Dermatol. Sci.* **2017**, *88*, 57–66; c) Q. Li, H. Fang, E. Dang, G. Wang, *J. Dermatol. Sci.* **2020**, *97*, 2–8; d) Y. Uchida, K. Park, *Am. J. Clin. Dermatol.* **2021**, *22*, 853–866.
- [5] a) O. Macheleidt, H. W. Kaiser, K. Sandhoff, *J. Invest. Dermatol.* **2002**, *119*, 166–173; b) J. Ishikawa, H. Narita, N. Kondo, M. Hotta, Y. Takagi, Y. Masukawa, T. Kitahara, Y. Takema, S. Koyano, S. Yamazaki, A. Hatamochi, *J. Invest. Dermatol.* **2010**, *130*, 2511–2514.
- [6] a) A. H. Merrill Jr, *Chem. Rev.* **2011**, *111*, 6387–6422; b) T. D. Mullen, Y. A. Hannun, L. M. Obeid, *Biochem. J.* **2012**, *441*, 789–802; c) M. Maceyka, S. Spiegel, *Nature* **2014**, *510*, 58–67; d) M. Rabionet, K. Gorgas, R. Sandhoff, *Biochim. Biophys. Acta* **2014**, *1841*, 422–434.
- [7] N. Coant, W. Sakamoto, C. Mao, Y. A. Hannun, *Adv. Biol. Regul.* **2017**, *63*, 122–131.
- [8] a) Y. A. Hannun, L. M. Obeid, *Nat. Rev. Mol. Cell Biol.* **2008**, *9*, 139–150; b) G. Napolitano, M. Karin, *Sci. Signaling* **2010**, *3*, pe34; c) T. Hla, A. J. Dannenberg, *Cell Metab.* **2012**, *16*, 420–434; d) B. Ogretmen, *Nat. Rev. Cancer* **2018**, *18*, 33–50.
- [9] a) A. Oizumi, H. Nakayama, N. Okino, C. Iwahara, K. Kina, R. Matsumoto, H. Ogawa, K. Takamori, M. Ito, Y. Suga, K. Iwabuchi, *PLoS One* **2014**, *9*, e89402; b) Y. Uchida, Y. I. Kim, K. Park, *Dermatol. Sin.* **2015**, *33*, 78–83; c) S. Bock, A. Pfalzgraff, G. Weindl, *J. Dermatol. Sci.* **2016**, *82*, 9–17; d) S. Igawa, J. E. Choi, Z. Wang, Y. L. Chang, C. C. Wu, T. Werbel, A. Ishida-Yamamoto, A. Di Nardo, *J. Invest. Dermatol.* **2019**, *139*, 1743–1752; e) K. Masuda-Kuroki, A. Di Nardo, *Biology* **2022**, *11*, 809; f) B. Kleuser, W. Bäumer, *Int. J. Mol. Sci.* **2023**, *24*, 1456.
- [10] a) J. Arikawa, M. Ishibashi, M. Kawashima, Y. Takagi, Y. Ichikawa, G. Imokawa, *J. Invest. Dermatol.* **2002**, *119*, 433–439; b) M. J. Choi, H. I. Maibach, *Am. J. Clin. Dermatol.* **2005**, *6*, 215–223; c) W. Sun, R. Xu, W. Hu, J. Jin, H. A. Crellin, J. Bielawski, Z. M. Szulc, B. H. Thiers, L. M. Obeid, C. Mao, *J. Invest. Dermatol.* **2008**, *128*, 389–397; d) K. Liakath-Ali, V. E. Vancollie, C. J. Lelliott, A. O. Speak, D. Lafont, H. J. Protheroe, C. Ingvorsen, A. Galli, A. Green, D. Gleeson, E. Ryder, L. Glover, G. Vizcay-Barrena, N. A. Karp, M. J. Arends, T. Brenn, S. Spiegel, D. J. Adams, F. M. Watt, L. van der Weyden, *J. Pathol.* **2016**, *239*, 374–383; e) R. Xu, P. Antwi Boasiako, C. Mao, *Cell. Signalling* **2021**, *78*, 109860.
- [11] Y. Ohnishi, N. Okino, M. Ito, S. Imayama, *Clin. Diagn. Lab. Immunol.* **1999**, *6*, 101–104.
- [12] N. Okino, M. Tani, S. Imayama, M. Ito, *J. Biol. Chem.* **1998**, *273*, 14368–14373.
- [13] T. Inoue, N. Okino, Y. Kakuta, A. Hijikata, H. Okano, H. M. Goda, M. Tani, N. Sueyoshi, K. Kambayashi, H. Matsumura, Y. Kai, M. Ito, *J. Biol. Chem.* **2009**, *284*, 9566–9577.
- [14] a) K. Kita, N. Sueyoshi, N. Okino, M. Inagaki, H. Ishida, M. Kiso, S. Imayama, T. Nakamura, M. Ito, *Biochem. J.* **2002**, *362*, 619–626; b) J. A. Geoghegan, A. D. Irvine, T. J. Foster, *Trends Microbiol.* **2018**, *26*, 484–497; c) A. L. Byrd, C. Deming, S. K. B. Cassidy, O. J. Harrison, W. I. Ng, S. Conlan, Y. Belkaid, J. A. Segre, H. H. Kong, *Sci. Transl. Med.* **2017**, *9*, eaal4651.
- [15] M. Sinha, N. Ghosh, D. S. Wijesinghe, S. S. Mathew-Steiner, A. Das, K. Singh, M. E. Masry, S. Khanna, H. Inoue, K. Yamazaki, M. Kawada, G. M. Gordillo, S. Roy, C. K. Sen, *Ann. Surg.* **2023**, *277*, e634–e647.
- [16] a) J. Jneid, J. P. Lavigne, B. La Scola, N. Cassir, *Hum. Microbiome J.* **2017**, *5–6*, 1–6; b) M. Loesche, S. E. Gardner, L. Kalan, J. Horwinski, Q. Zheng, B. P. Hodkinson, A. S. Tyldsley, C. L. Franciscus, S. L. Hillis, S. Mehta, D. J. Margolis, E. A. Grice, *J. Invest. Dermatol.* **2017**, *137*, 237–244; c) D. Lebowitz, K. Gariani, B. Kressmann, E. Von Dach, B. Huttner, P. Bartolone, N. Le, M. Mohamad, B. A. Lipsky, I. Uckay, *Int. J. Infect. Dis.* **2017**, *59*, 61–64; d) L. R. Kalan, J. S. Meisel, M. A. Loesche, J. Horwinski, I. Soaita, X. Chen, A. Uberoi, S. E. Gardner, E. A. Grice, *Cell Host Microbe* **2019**, *25*, 641–655; e) Y. K. Wu, N. C. Cheng, C. M. Cheng, *Trends Biotechnol.* **2019**, *37*, 505–517.
- [17] a) W. J. Jeffcoate, K. G. Harding, *Lancet* **2003**, *361*, 1545–1551; b) D. G. Armstrong, A. J. Boulton, S. A. Bus, *N. Engl. J. Med.* **2017**, *376*, 2367–2375; c) W. J. Jeffcoate, L. Vileikyte, E. J. Boyko, D. G. Armstrong, A. J. M. Boulton, *Diabetes Care* **2018**, *41*, 645–652.
- [18] M. Tani, N. Okino, S. Mitsutake, M. Ito, *J. Biochem.* **1999**, *125*, 746–749.
- [19] M. Casasampere, L. Camacho, F. Cingolani, J. Casas, M. Egidio-Gabas, J. L. Abad, C. Bedia, R. Xu, K. Wang, D. Canals, Y. A. Hannun, C. Mao, G. Fabrias, *J. Lipid Res.* **2015**, *56*, 2019–2028.
- [20] a) E. M. Saied, C. Arenz, *Chem. Phys. Lipids* **2016**, *197*, 60–68; b) Y. Otsuka, M. V. Airola, Y. M. Choi, N. Coant, J. Snider, C. Cariello, E. M. Saied, C. Arenz, T. Bannister, R. Rahaim Jr, Y. A. Hannun, J. Shumate, L. Scampavia, J. D. Haley, T. P. Spicer, *SLAS Discov.* **2021**, *26*, 113–121.
- [21] R. S. Magin, X. Liu, A. Felix, A. S. Bratt, W. C. Chan, S. J. Buhrlage, *Cell Chem. Biol.* **2021**, *28*, 1090–1100.
- [22] E. A. Grice, H. H. Kong, S. Conlan, C. B. Deming, J. Davis, A. C. Young, G. G. Bouffard, R. W. Blakesley, P. R. Murray, E. D. Green, M. L. Turner, J. A. Segre, *Science* **2009**, *324*, 1190–1192.
- [23] S. E. Bawab, J. Usta, P. Roddy, Z. M. Szulc, A. Bielawska, Y. A. Hannun, *J. Lipid Res.* **2002**, *43*, 141–148.
- [24] C. Peters, A. Billich, M. Ghobrial, K. Högenauer, T. Ullrich, P. Nussbaumer, *J. Org. Chem.* **2007**, *72*, 1842–1845.
- [25] a) Y. Xu, M. S. Hixon, P. E. Dawson, K. D. Janda, *J. Org. Chem.* **2007**, *72*, 6700–6707; b) S. Ohayon, L. Spasser, A. Aharoni, A. Brik, *J. Am. Chem. Soc.* **2012**, *134*, 3281–3289.
- [26] T. Pinkert, D. Furkert, T. Korte, A. Herrmann, C. Arenz, *Angew. Chem. Int. Ed.* **2017**, *56*, 2790–2794.
- [27] T. K. M. Nguyen, M. R. Ki, R. G. Son, S. P. Pack, *Appl. Microbiol. Biotechnol.* **2019**, *103*, 2205–2216.
- [28] a) H. Inoue, T. Someno, T. Kato, H. Kumagai, M. Kawada, D. Ikeda, *J. Antibiot.* **2009**, *62*, 63–67; b) H. Inoue, T. Someno, M. Kawada, D. Ikeda, *J. Antibiot.* **2010**, *63*, 611–613.
- [29] M. S. Finnin, J. R. Donigian, A. Cohen, V. M. Richon, R. A. Rifkind, P. A. Marks, R. Breslow, N. P. Pavletich, *Nature* **1999**, *401*, 188–193.
- [30] R. D. Healey, E. M. Saied, X. Cong, G. Karsai, L. Gabellier, J. Saint-Paul, E. Del Nero, S. Jeannot, M. Drapeau, S. Fontanel, D. Maurel, S. Basu, C. Leyrat, J. Golebiowski, G. Bossis, C. Bechara, T. Hornemann, C. Arenz, S. Granier, *Angew. Chem. Int. Ed.* **2022**, *61*, e202109967.
- [31] a) N. Bielsa, M. Casasampere, M. Aseeri, J. Casas, A. Delgado, J. L. Abad, G. Fabrias, *Eur. J. Med. Chem.* **2021**, *216*, 113296; b) K. P. Bhabak, C. Arenz, *Bioorg. Med. Chem.* **2012**, *20*, 6162–6170; c) K. P. Bhabak, B. Kleuser, A. Huwiler, C. Arenz, *Bioorg. Med. Chem.* **2013**, *21*, 874–882.
- [32] M. V. Airola, W. J. Allen, M. J. Pulkoski-Gross, L. M. Obeid, R. C. Rizzo, Y. A. Hannun, *Structure* **2015**, *23*, 1482–1491.
- [33] a) C. M. Ouairy, M. J. Ferraz, R. G. Boot, M. P. Baggelaar, M. van der Stelt, M. Appelman, G. A. van der Marel, B. I. Florea, J. M. Aerts, H. S. Overkleeft, *Chem. Commun.* **2015**, *51*, 6161–6163; b) Y. F. Ordóñez, J. L. Abad, M. Aseeri, J. Casas, V. Garcia, M. Casasampere, E. H. Schuchman, T. Levade, A. Delgado, G. Triola, G. Fabrias, *J. Am. Chem. Soc.* **2019**, *141*, 7736–7742.

- [34] D. Pizzirani, A. Bach, N. Realini, A. Armirotti, L. Mengatto, I. Bauer, S. Girotto, C. Pagliuca, M. De Vivo, M. Summa, A. Ribeiro, D. Piomelli, *Angew. Chem. Int. Ed.* **2015**, *54*, 366.
- [35] a) Z. Li, P. Hao, L. Li, C. Y. J. Tan, X. Cheng, G. Y. J. Chen, S. K. Sze, H. M. Shen, S. Q. Yao, *Angew. Chem. Int. Ed.* **2013**, *52*, 8551–8556; b) H. Park, J. Y. Koo, Y. V. Srikanth, S. Oh, J. Lee, J. Park, S. B. Park, *Chem. Commun.* **2016**, *52*, 5828–5831; c) L. P. Conway, A. M. Jadhav, R. A. Homan, W. Li, J. S. Rubiano, R. Hawkins, R. M. Lawrence, C. G. Parker, *Chem. Sci.* **2021**, *12*, 7839–7847; d) I. V. L. Wilkinson, M. Bottlinger, Y. El Harraoui, S. A. Sieber, *Angew. Chem. Int. Ed.* **2023**, *62*, e202212111.
- [36] a) A. E. LaBauve, M. J. Wargo, *PLoS Pathog.* **2014**, *10*, e1003889; b) N. Okino, M. Ito, *Sci. Rep.* **2016**, *6*, 38797.

Manuscript received: May 30, 2023

Accepted manuscript online: June 20, 2023

Version of record online: July 10, 2023